ARTICLES

Dipole−Dipole Interactions in Spin-Labeled Au Nanoparticles as a Measure of Interspin Distances

Petre Ionita,[†] Agneta Caragheorgheopol,[‡] Bruce C. Gilbert,[†] and Victor Chechik*[,†]

Department of Chemistry, University of York, Heslington, York YO10 5DD, U.K., and Romanian Academy, Institute of Physical Chemistry "I. G. Murgulescu", Spl. Independentei 202, 77208 Bucharest, Romania

Received: September 22, 2004; In Final Form: December 21, 2004

A series of Au nanoparticles modified with a nitroxide-functionalized ligand was prepared with a range of spin-label coverage. The X-band EPR spectra of frozen solutions of these nanoparticles showed coverage-dependent line-broadening due to dipole−dipole interactions between spin labels. We developed a methodology to analyze such spectra in terms of geometrical features of the nanoparticles (e.g., Au core size and the length of the spin-labeled ligand). Our method is based on the assumption that the spectral line shape is determined by the average distance between nearest-neighboring spin labels adsorbed on the Au particle. Geometrical and statistical analysis then relates this distance to the line shape parameter d_1/d, which was calibrated using a model system. Application of this methodology to the experimental spectra provided information about the conformation of ligands on the Au surface. We found that, if the spin-labeled ligand is substantially longer than the surrounding protecting layer, it does not adopt a fully stretched conformation but wraps around the particle immediately above the layer of surrounding ligand. Our results also show that the ligands do not adsorb cooperatively on the Au surface.

I. Introduction

Thiol-protected Au nanoparticles have been an extremely popular subject of studies[1] since the discovery of an efficient method for their preparation by Schiffrin et al.[2] This is partly due to the wide range of potential applications of nanostructured materials. Au nanoparticles, however, also represent one of the simplest-to-synthesize and best-defined large supramolecular assemblies, and hence, understanding their properties is of a substantial fundamental interest.

A number of research groups have explored the arrangement of the organic layers in Au nanoparticles. Most studies focused on determining the degree of order in well-packed layers of long-chain alkanethiols on the Au surface. For instance, FT-IR and ^{13}C NMR measurements showed that, for the nanoparticles protected by long-chain thiols ($>C_{16}$), the alkane chains exist predominantly in an all-trans conformation. Shorter-chain thiol-protected particles are less well-packed, and the order−disorder transition in these materials was explored in temperature-dependent NMR studies.[3] Site-specific ^2H labeling allowed the dynamics of the organic layer to be probed by FT-IR and ^2H NMR. These studies showed a lack of mobility around the carbon atom closest to the metal surface on the millisecond time scale at 25 °C.[4] The mobility increased progressively with the distance between the functional group and the Au surface.

Unlike the average packing of ligands, their distribution on the surface of Au nanoparticles is much harder to probe. There is some circumstantial evidence for the presence of several different types of binding site which possess different reactivity.[5] This was tentatively attributed to the presence of defect sites on the nanoparticle surface.[6] Alternatively, the edge, vertex, and terrace sites on the surface of faceted Au nanoparticles could possess different reactivities.[7] The distribution of ligands on the nanoparticle surface, however, is difficult to study; most directly, this could be probed by analytical techniques sensitive to the distance between the ligands.

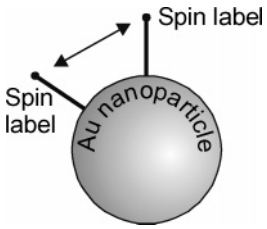

Figure 1. Schematic drawing of an Au nanoparticle modified with two spin-labeled ligands.

Electron paramagnetic resonance (EPR) of spin labels is one such technique. The continuous wave (CW)-EPR spectrum of a spin label is sensitive to the presence of another spin label within the radius of ca. 3 nm.[8] Two major mechanisms of spin−spin interaction account for this sensitivity: exchange and dipole−dipole interaction. Exchange interaction usually operates through collisions of spin-bearing functionalities and thus is mostly observed in low-viscosity, fast-tumbling systems. Dipole−dipole interaction, on the other hand, is averaged out to zero in fast-tumbling systems and is therefore usually observed only in the powder spectra of frozen solutions.

Recently, we exploited the exchange interaction in diradical ligands in a mechanistic study of the ligand-exchange reaction

* Corresponding author. E-mail address: vc4@york.ac.uk.
[†] University of York.
[‡] Romanian Academy.

10.1021/jp045696n CCC: $30.25
Published on Web 02/11/2005

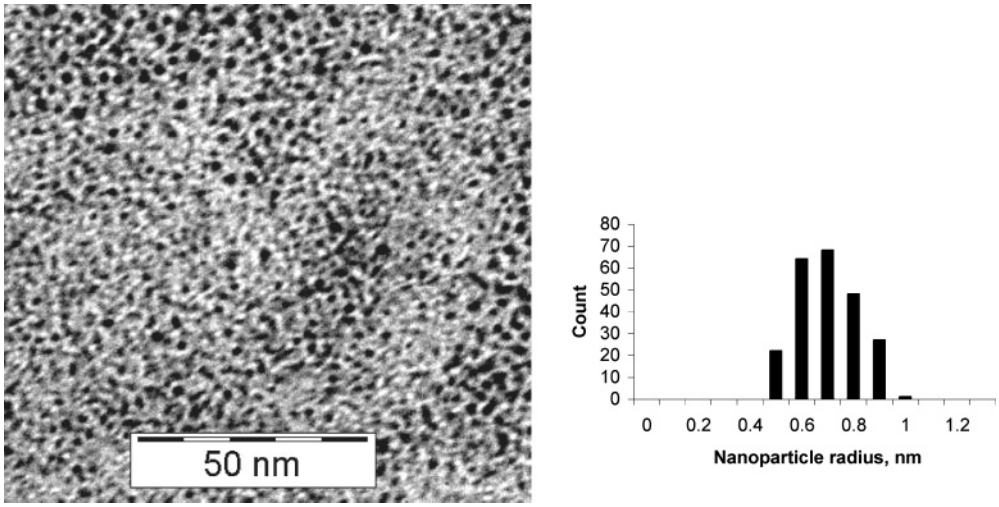

Figure 2. A typical TEM image of spin-labeled nanoparticles **3a** and the corresponding size distribution histogram. Average nanoparticle radius was 0.65 ± 0.12 nm.

SCHEME 1: Preparation of Spin-Labeled Au Nanoparticles 3a,b

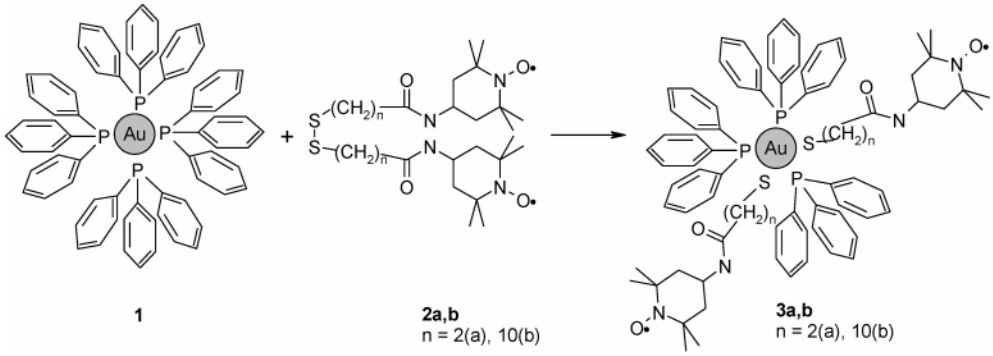

with Au nanoparticles. We have found that this reaction could be conveniently used to prepare spin-labeled Au nanoparticles with a wide range of spin-label coverage.[9] The ligand exchange reaction with disulfide ligands leads to the separation of the two branches of the disulfide molecule; the two branches do not adsorb next to each other on the Au surface.[6,10]

The aim of this study was to explore the dipole−dipole interactions between multiple spin labels adsorbed on the same Au nanoparticle (Figure 1). Quantitative analysis of these interactions could provide information about the distribution of the spin labels on the nanoparticle surface and the conformation of the adsorbed ligands. This will be achieved by the analysis of X-band powder EPR spectra of spin-labeled nanoparticles in frozen solutions.

II. Results

A. Preparation Of Spin-Labeled Au Nanoparticles. Spin-labeled Au nanoparticles were prepared by an exchange reaction of triphenylphosphine-protected particles **1** with disulfides **2a**,**b** as described elsewhere (Scheme 1).[9] High-coverage spin-labeled nanoparticles were purified by gel permeation chromatography (GPC) to remove unreacted disulfide. For particles with lower coverage (up to an average coverage of five spin labels per particle), this was not necessary; a control experiment showed the absence of unreacted spin labels. We previously had found that different preparations of Au nanoparticles (particularly with a different aging history) sometimes show different properties.[11] All EPR studies described in this paper were hence carried out with the same batch of Au nanoparticles in a short period of time, to reduce aging effects.

The nanoparticles were characterized by transmission electron microscopy (TEM) (Figure 2). The particle size and size distribution were consistent with the literature reports.[12] A control experiment showed that the particle size remained unchanged after the exchange reaction. The amount of spin label for the lower-coverage particle was determined by the stoichiometry of the exchange reaction; the validity of this was proven by double integration of an EPR spectrum of a control sample. The composition of the high-coverage Au nanoparticles (purified by GPC) was determined by recording their spectra together with the spectra of 2,2,6,6-tetramethylpiperidinyl-1-oxyl (TEMPO) solutions of known concentrations in a dual cavity and comparing the double integrals. The amount of Au in the latter samples was quantified by inductively coupled plasma optical emission spectroscopy (ICP−OES) analysis following digestion of the Au nanoparticles in aqua regia.

B. Au Nanoparticles with High Coverage Of Spin Label. X-band EPR spectra of frozen solutions of spin-labeled Au nanoparticles **3a**,**b** with high coverage (>seven spin labels per particle) are shown in Figure 3a,b, respectively. The spectra were recorded as dilute frozen solutions in 20% dichloromethane (DCM)/toluene at 110 K. One can observe that with increased average coverage $\bar{y}$ the line shape gradually changes from a typical pattern of isolated nitroxide (three lines) to a spectral pattern dominated by a single broad line. This is due to dipole−dipole and exchange interactions between adjacent nitroxides adsorbed on the same nanoparticle. Stronger interactions at higher coverage lead to the increased contribution of the broad line.

It is interesting to compare the EPR line shape for Au nanoparticles coated with short-chain (Figure 3a) and long-chain

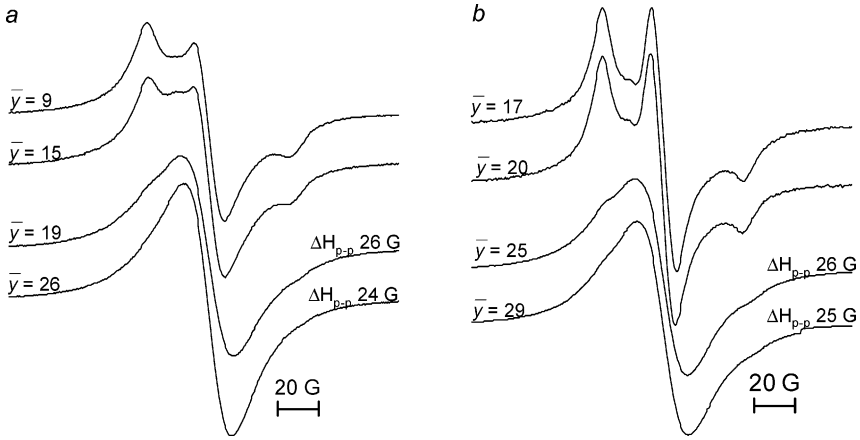

Figure 3. X-band EPR spectra of frozen solutions of spin-labeled Au nanoparticles **3a** (a) and **3b** (b), normalized by the spin count. The spectra were recorded in 20% DCM/toluene at 110 K. The numbers above the curves show the average coverage of spin labels per nanoparticle $\bar{y}$ and peak-to-peak line widths of the broad line ΔH_{p-p}. The average coverage was calculated using eq 9, vide infra.

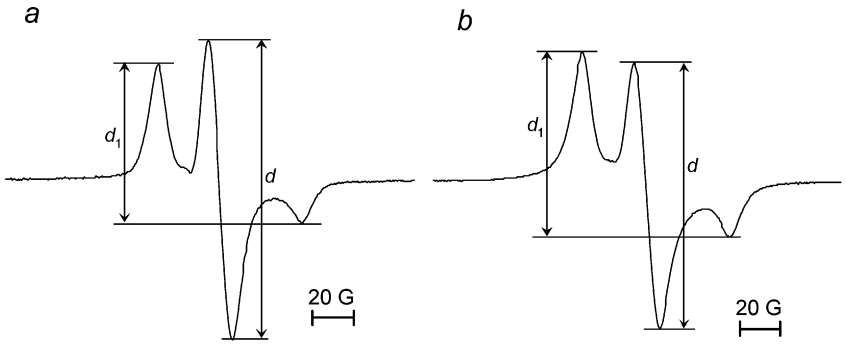

Figure 4. EPR spectra of frozen solutions of spin-labeled Au nanoparticles **3a** at 0.1 (a) and 5 (b) spin labels per nanoparticle, respectively. The spectra were run in 20% DCM/toluene at 110 K.

(Figure 3b) nitroxides. At similar coverage, the relative contribution of the broad line to the overall spectra is somewhat less important for the nanoparticles **3b** (coated with a long-chain nitroxide). This is probably due to the curvature of the nanoparticle surface. As the nitroxide functionalities in **3b** are further away from the particle center, the average distance between adjacent nitroxides is likely to be larger compared to nanoparticles **3a**. The larger the interspin distance is, the weaker the spin−spin interactions, and hence, the smaller the contribution of the broad line.

Similar arguments can be applied to the line width of the high-coverage nanoparticle spectra. The increased coverage leads to the narrowing of the broad line (an effect similar to exchange narrowing observed in the spectra of neat nitroxides). The peak-to-peak line width ΔH_{p-p} is smaller for the shorter chain nitroxide particles **3a** compared to a similar coverage particles **3b** (Figure 3a,b), consistent with the smaller interspin distance. Interestingly, the room-temperature solution spectra of nanoparticles **3a**,**b** are also dominated by a broad line; the line width in the latter case, however, is substantially smaller (ca. 15 G).[9] The narrowing of the line at room temperature is due to the averaging of the dipole−dipole interactions and the higher contribution of the exchange interaction caused by the frequent collisions between nitroxides in a fluid solution.

The degree of packing of nitroxides on the surface can be estimated by comparing the line width of the broad line to related systems. For instance, Risse et al. examined self-assembled films of spin-labeled stearic acid adsorbed on Al_2O_3. At full coverage, the spectra were dominated by a broad line with ΔH_{p-p} of 19 G, a value close to that of the neat spin label.[13] This indicated a high degree of packing in the monolayers. In our case, the neat nitroxides **2a**,**b** showed spectra with ΔH_{p-p} of ca. 11−13 G, substantially less than the line width of spin-labeled nanoparticle spectra. This suggests a relatively loose packing of the nitroxide ligands on the nanoparticle surface, probably due to the curvature of the surface and incomplete exchange reaction, which prevents the formation of a full monolayer of the spin label on the Au nanoparticle surface. Unfortunately, because of the complexity of interactions in this system, no further quantitative information could be obtained from the EPR spectra of high-coverage spin-labeled nanoparticles.

C. Au Nanoparticles with Medium Coverage of Spin Label. The X-band EPR spectra of frozen solutions of medium-coverage spin-labeled Au nanoparticles show hyperfine structure (Figure 4). The line shape changes substantially as a function of coverage. This effect can be attributed to the coverage-dependent dipole−dipole interaction between adjacent spins adsorbed on the same nanoparticle. Two approaches can be used to analyze the contribution of the dipole−dipole interactions to such spectra. In the first approach, the spectral line shape is simulated by convoluting the spectrum of an isolated spin label (e.g., with no dipole−dipole contribution) with the distribution function of spin labels in the sample.[14,15] The second approach relies on an empirically found spectral parameter, the ratio of the peak heights d_1/d (Figure 4), which is sensitive to the distance between interacting spins. This parameter was first introduced by Russian scientists in the 1970s. To a good approximation, it is inversely proportional to the distance between interacting spins in both rigid molecules and structures with a random distribution of spins in space.[16] The validity of this empirical equation has been confirmed for a broad range of spin-labeled systems. The d_1/d parameter is therefore a convenient measure of the dipole−dipole broadening effect. In

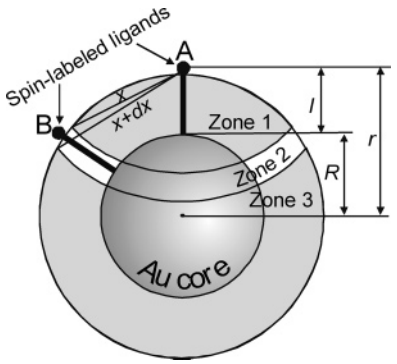

Figure 5. Geometric parameters of spin-labeled Au nanoparticles.

this study, we chose this parameter to characterize the strength of dipole−dipole interactions. Because of the complexity of our system (e.g., statistical distribution of Au nanoparticle sizes and spin labels on the particles, dipole−dipole interactions in groups of more than two spin labels, etc.), we felt that the use of d_1/d parameters is more appropriate than spectra simulation.

If a random distribution of spin labels on nanoparticles is assumed, the distances between adsorbed spin labels (and hence the strength of dipole−dipole interactions) are determined by the following geometric parameters (Figure 5): (a) average nanoparticle size ($\bar{R}$) and the shape of size distribution, (b) elemental composition of the nanoparticles, for example, the number of spin labels per Au atom (N_r/N_{at}), and (c) the average distance between the nitroxides and the Au surface (l). The information about Au core size distribution can be obtained from the TEM images (e.g., Figure 2), and the elemental composition of the nanoparticles can be calculated from the exchange reaction stoichiometry. The only unknown parameter which affects the strength of dipole−dipole interactions is hence the distance between the nitroxide and the Au surface (l). Analysis of the powder EPR spectra of spin-labeled nanoparticles therefore makes it possible to find this parameter, which provides direct information about the conformation of spin labels adsorbed on Au nanoparticles. The conformations of supramolecular assemblies in solution are very difficult to study by other methods, and it is the aim of this section to develop analysis of powder EPR spectra which would characterize the arrangement of ligands on the surface of Au nanoparticles.

Dipole−Dipole Interaction Model. Following literature precedent,[14] we assumed that dipole−dipole interactions in the spin-label assemblies are dominated by the interactions between nearest neighbors. To develop a mathematical procedure, which could simulate the effect of dipole−dipole interactions on the spectra of spin-labeled nanoparticles, we carried out the following steps:

(a) Calibrated d_1/d parameter as a function of average distance $\bar{x}$ between nearest-neighboring spins using a system with a known distribution of spin labels. We used frozen solutions of TEMPO with known concentrations as such a model system. Using this calibration, we then calculated the $\bar{x}_{exp}$ values for the spin-labeled nanoparticles with different size/coverage from the experimental d_1/d parameters.

(b) Derived an analytical expression which gives the average distance $\bar{x}$ between nearest-neighboring spin labels adsorbed on an Au nanoparticle as a function of particle size (R), length of the ligand (l), and the number of spin labels per particle (y) (Figure 5).

(c) Chose probability density functions to describe the distribution of Au particle sizes and the distribution of the number of spin labels per particle.

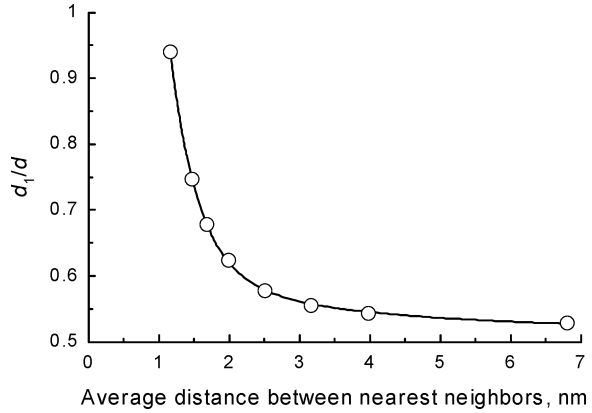

Figure 6. A calibration plot of d_1/d parameter vs average nearest-neighbor distance $\bar{x}$ obtained from powder EPR spectra of TEMPO solutions. The solid line is a best fit of experimental data using eq 2.

(d) Determined how to combine d_1/d values for contributions from different Au nanoparticles.

These steps allowed us to predict the d_1/d values for an assembly of spin-labeled nanoparticles as a function of the average Au core size $\bar{R}$ and the standard deviation σ, the average elemental composition of nanoparticles (relative number of spin labels per Au atom N_r/N_{at}), and the distance between the nitroxide group and the Au surface l. The rest of this section considers each step in detail.

Calibration of d_1/d Parameter Using Frozen TEMPO Solutions. We recorded a series of powder EPR spectra of TEMPO solutions in 20% DCM/toluene at 110 K. The concentration of TEMPO was varied in a broad range. The average distance between nearest-neighboring nitroxides, $\bar{x}$'s, in these solutions could be calculated from the concentration of spin labels using eq 1.[17]

$$\bar{x} = \Gamma\left(\frac{4}{3}\right)\sqrt[3]{\frac{3}{4\pi s}} \qquad (1)$$

Here, Γ is gamma function, and s is the number of spin-label molecules per unit volume (which is easily derived from the concentration of spin labels). This equation is true for a random distribution of spins in bulk solutions. The d_1/d parameters measured from the experimental spectra were then plotted against average nearest-neighbor distances $\bar{x}$'s calculated using eq 1 (Figure 6). This calibration curve is very similar to those reported in the literature.[16]

The data in Figure 6 were fitted to an empirical eq 2. The values of empirical parameters a_1-a_5 were 0.8050, 3.0150 nm^{-1}, 0.8736 nm, 0.5145, and 0.06824 nm, respectively, as obtained by nonlinear regression.

$$d_1/d = a_1 e^{-a_2(\bar{x}-a_3)} + a_4 + \frac{a_5}{\bar{x}} \qquad (2)$$

Equation 2 is a purely empirical function which we used to approximate the relationship d_1/d versus $\bar{x}$. It has no physical meaning and represents a more complex alternative to similar empirical relationships found in the literature;[16] it fits the experimental data better but gives very similar results. Using this equation and experimental d_1/d values for spin-labeled nanoparticles **3a**,**b** with different coverages, we calculated the average distances between nearest-neighboring spin labels (Table 1).

The interspin distances in Table 1 decrease with increased coverage of spin label. The values for lowest coverage in Table

TABLE 1: Empirical Parameter d_1/d and Average Distances between Nearest-Neighboring Spin Labels $\bar{x}_{exp}$'s, Calculated from the Calibration Curve (Eq 2)

spin labels per Au atom (N_r/N_{at})	nanoparticles **3a**		nanoparticles **3b**	
	d_1/d	$\bar{x}_{exp}$, nm	d_1/d	$\bar{x}_{exp}$, nm
0.0012	0.54	3.35	0.53	4.20
0.0048	0.55	2.34	0.51	
0.0083	0.55	2.41	0.54	2.91
0.012	0.59	1.91	0.56	2.22
0.019	0.61	1.78	0.60	1.84
0.024	0.63	1.68	0.61	1.78
0.030	0.64	1.62	0.62	1.69
0.036	0.66	1.57	0.64	1.63
0.048	0.67	1.52	0.64	1.61
0.059	0.70	1.46	0.64	1.61

1 (e.g., first three rows), however, are probably not reliable, as the dipole−dipole interaction for interspin distances in these samples are too weak to give accurate data.[18]

Mathematical Analysis of the Average Distance between Nearest Neighbors. To analyze the distances $\bar{x}_{exp}$'s in Table 1 in terms of geometric parameters of the Au nanoparticle (e.g., particle radius R and the length of the ligand l), one has to consider a basic mathematical problem: what is the average distance between nearest neighbors for randomly scattered points on the surface of a sphere? We solved this problem using an approach similar to that reported by Scott and Tout.[19] Let us consider a nanoparticle containing y randomly distributed spin labels (Figure 5). The distance from the nanoparticle center to the spin label is defined as r. Let us further define function $w(x)\,dx$ as the probability that, for a given spin label A, the distance to the nearest neighbor B is between x and $x + dx$. On the other hand, this probability equals the probability that there is a spin label in zone 2 times the probability that all other spin labels are in zone 3 (Figure 5). The probability that there is a spin label in zone 2 equals the ratio of the area of zone 2 to the overall area of the nanoparticle multiplied by the number of remaining spin labels ($y - 1$) (this is only true for an infinitesimally small zone 2; see Supporting Information for more details). Similarly, the probability that all other ($y - 2$) spin labels are in zone 3 equals the ratio of the area of zone 3 to the overall area of nanoparticle raised to the power of ($y - 2$). Using simple geometric transformations, we can then write eq 3

$$w(x)\,dx = \frac{y-1}{2^{2y-3}r^{2y-2}}\,x(4r^2 - x^2)^{y-2}\,dx \tag{3}$$

The average distance between the nearest neighbors $\bar{x}$ on the nanoparticle equals $\int_0^{2r} xw(x)\,dx$. Integration using eq 3 then gives the desired function (eq 4). Further details can be found in the Supporting Information.

$$\bar{x} = \int_0^{2r} xw(x)\,dx = \sqrt{\pi}r\,\frac{\Gamma(y)}{\Gamma(y+0.5)} \tag{4}$$

Statistical Distributions. Formula 4 describes the average distance between nearest-neighboring spin labels for a given nanoparticle with radius r, modified with y spin labels. However, the nanoparticles used in this study are polydisperse. Moreover, as we assumed a random distribution of spin labels on particles, even particles of the same size may have different numbers of spin labels. We must therefore consider the distribution of particle sizes, and for particles of a given size, the distribution of spin labels on their surfaces.

The particle size distribution can be assumed to have a Gaussian shape; the average nanoparticle radius $\bar{R}$ and the standard deviation σ can be calculated from the TEM images (Figure 2). The probability $p_R\,dR$ of finding a particle with the radius between R and $R + dR$ can therefore be determined from eq 5

$$p_R\,dR = \frac{1}{\sigma\sqrt{2\pi}}\,e^{-(R-\bar{R})^2/2\sigma^2}\,dR \tag{5}$$

To analyze the distribution of spin labels, we need to determine the average number of spin labels on a particle of a given radius R. The number of Au atoms in a particle with the core radius R can be calculated as $^4/_3\pi R^3\bar{n}_{Au}^{fcc}$, where $\bar{n}_{Au}^{fcc}$ is the packing density of Au atoms in an fcc lattice.[20] If a Gaussian distribution of particle sizes is assumed, the total number of Au atoms can be calculated using eq 6[21]

$$N_{at} = \int_{-\infty}^{\infty} \frac{4}{3}\pi R^3\bar{n}_{Au}^{fcc}\cdot N_p\cdot\frac{e^{-(R-\bar{R})^2/2\sigma^2}}{\sigma\sqrt{2\pi}}\,dR \tag{6}$$

Here, N_p is the overall number of Au particles. Integration of eq 6 and solving for N_p gives eq 7

$$N_p = \frac{3N_{at}}{4\pi\bar{n}_{Au}^{fcc}(3\sigma^2\bar{R} + \bar{R}^3)} \tag{7}$$

Similarly, the total surface area A of all nanoparticles is given by eq 8, which can be integrated after the substitution of eq 7.

$$A = \int_{-\infty}^{\infty} 4\pi R^2\cdot N_p\cdot\frac{e^{-(R-\bar{R})^2/2\sigma^2}}{\sigma\sqrt{2\pi}}\,dr = \frac{3N_{at}(\sigma^2 + \bar{R}^2)}{\bar{n}_{Au}^{fcc}(3\sigma^2\bar{R} + \bar{R}^3)} \tag{8}$$

The average surface density of spin labels in nanoparticles is the ratio of the number of spin labels N_r over the area A. For any nanoparticle with radius R, the average coverage $\bar{y}$ (e.g., the number of spin labels per particle) equals the average surface density times the surface area of this nanoparticle (eq 9).

$$\bar{y} = 4\pi R^2\,\frac{N_r}{A} = \frac{N_r}{N_{at}}\cdot\frac{4\pi R^2\bar{n}_{Au}^{fcc}(3\sigma^2\bar{R} + \bar{R}^3)}{3(\sigma^2 + \bar{R}^2)} \tag{9}$$

The overall numbers of Au atoms N_{at} and spin labels N_r in the sample are known from the elemental analysis (performed with ICP−OES) and double integration of the EPR spectra, respectively. Equation 9 therefore allows us to calculate the average coverage of spin labels as a function of nanoparticle radius R. The number of spin labels on a given nanoparticle, however, may vary from 0 to n, where n is the number of Au atoms at the nanoparticle surface. The value of n can be estimated using eq 10 (R_{Au} is the radius of the Au atom; full derivation of eq 10 is given in the Supporting Information).

$$n = \frac{4}{3}\pi\bar{n}_{Au}^{fcc}\left[R^3 - \left(R - \frac{2\sqrt{6}}{3}R_{Au}\right)^3\right] \tag{10}$$

A random distribution of spin labels on the particles is given by a binomial distribution. Equations 9 and 10 can then be used to determine the probability p_y of finding a particle with any given number of spin labels y (eq 11).

$$p_y = {}^nC_y\left(\frac{\bar{y}}{n}\right)^y\left(1 - \frac{\bar{y}}{n}\right)^{n-y} \tag{11}$$

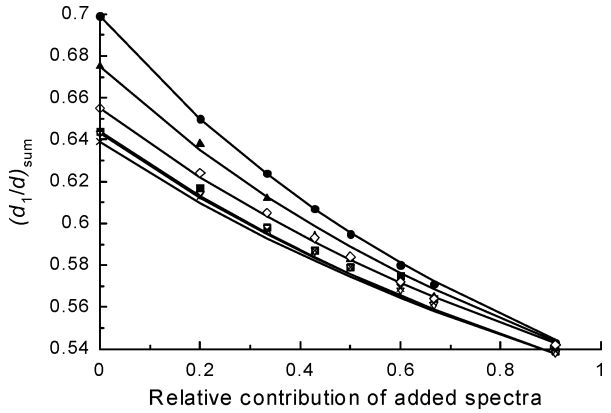

Figure 7. d_1/d parameters for the sum of two EPR spectra.

Additivity of d_1/d Parameters. Equations 2 and 4 allow us to calculate the d_1/d values for any given nanoparticle, and eqs 5, 9, 10, and 11 describe the probability of finding a nanoparticle with any given radius and number of spin labels. In a polydisperse system like ours, the spectra of individual nanoparticles add together to give the observed experimental spectrum. To calculate the d_1/d value for the observed spectrum, we must therefore combine these parameters for individual spectra. To a good approximation, the d_1/d parameter has been shown to be inversely proportional to the interspin distance x (or average interspin distance $\bar{x}$) for rigid diradicals and systems with a statistical distribution of radicals alike (e.g., $x = \alpha + \alpha_1/(d_1/d - \beta)$) where α, α_1, and β are constants.[16] For a two-component system, $\bar{x} = I_1x_1 + (1 - I_1)x_2$, where I_1 is the relative intensity of the first component. Combining these two identities, we obtain eqs 12 and 13

$$\bar{x} = \alpha + \alpha_1\left[\frac{I_1}{(d_1/d)_1 - \beta} + \frac{(1 - I_1)}{(d_1/d)_2 - \beta}\right] = \alpha + \frac{\alpha_1}{(d_1/d)_{ave} - \beta} \quad (12)$$

$$\frac{1}{(d_1/d)_{ave} - \beta} = \frac{I_1}{(d_1/d)_1 - \beta} + \frac{1 - I_1}{(d_1/d)_2 - \beta} \quad (13)$$

Therefore, to determine the d_1/d parameter for a sum of two EPR spectra, one could add inverse d_1/d values for individual components (corrected for the relative intensity) after subtracting a constant (β). To find the value of constant β, we recorded a series of EPR spectra of spin-labeled nanoparticles with coverage in the range 0.1−5 spin labels per particle. The pairs of experimental spectra were then added together using a range of their relative intensities. The d_1/d parameters for the sum spectrum were then fitted to the d_1/d parameters of the individual components using eq 13. By using nonlinear regression, constant β was found to be 0.307 (Figure 7). A good fit to the experimental data confirmed the validity of eq 13.

To further test the additivity of d_1/d values, we have simulated EPR spectra of monodisperse Au nanoparticles possessing one, two, four, or six spin labels. The simulations confirmed that d_1/d values are sensitive to the interspin distances up to 2−2.5 nm. The pairs of simulated spectra were then added in different proportions, and d_1/d values for these sums showed excellent agreement with the values predicted by eq 13. Further details can be found in the Supporting Information.

Simulation of d_1/d Parameters for Spin-Labeled Nanoparticles. We can now put together the overall procedure for calculating d_1/d parameters for the assembly of Au nanoparticles. Our method screens all particle radii from the radius of an Au atom R_{Au} to infinity. The contribution of each particle size is given by the Gaussian distribution (eq 5). For each particle size, the distribution of spin labels is determined by a normal distribution (eq 11). Finally, eq 13 is used to add together individual contributions for each particle size and for every possible number of spin labels per particle. These contributions are multiplied by the number of spin labels per particle to take into account that the intensity of the EPR spectra is proportional to the number of spins. The mathematical representation of this summation is given in eq 14

$$d_1/d = \beta + \frac{\int_{R_{Au}}^{\infty} \bar{y} \cdot p_R \cdot dR}{\int_{R_{Au}}^{\infty} \bar{y} \cdot p_R \cdot \frac{\sum_{y=1}^{n} y \cdot p_y \cdot [(d_1/d)_y - \beta]^{-1}}{\sum_{y=1}^{n} y \cdot p_y} \cdot dR} \quad (14)$$

We used eq 14 to calculate the d_1/d parameters for Au nanoparticles. The average coverage $\bar{y}$ and the number of surface Au atoms n were calculated for each particle size using eqs 9 and 10. The $(d_1/d)_y$ parameters for individual spectra were calculated using the calibration curve (eq 2); the $\bar{x}$ value required by this equation was calculated using formula 4. The variable r in eq 4 is the distance from the nanoparticle center to the spin label, which is a sum of the Au core radius R and the length of the spin label l (e.g., the distance between the nitroxide group and the Au surface): $r = R + l$. All the parameters in these equations are known except the length of the spin label. We therefore optimized this variable, l, to achieve the best fit of the calculated d_1/d parameters (eq 14) with the experimental values. This optimization procedure was carried out for spin-labeled Au nanoparticles **3a**,**b**. A good fit can only be obtained if the data points for the two highest coverages are ignored (vide infra). The calculated and experimental data are in Table 2, along with the average coverage which was calculated using eq 9 and assuming the normal distribution of nanoparticle sizes. The optimization gave the length of spin labels **2a**,**b**, as 0.80 and 0.88 nm, respectively.

III. Discussion

A. Conformation of Spin-Labeled Ligands on Au Nanoparticles. It is interesting to compare the calculated distance from the nitroxide group to the Au surface l for the spin-labeled particles **3a**,**b** (Table 2). The lengths of the fully stretched branches of disulfides **2a**,**b** are 1.2 and 2.2 nm, respectively (as determined from molecular models). These lengths are substantially larger than the calculated values of l (0.8 and 0.88 nm, Table 2). Despite the fact that disulfide **2b** is substantially longer than disulfide **2a**, the distance from the nitroxide group to the surface of the Au nanoparticle is only slightly greater. It is therefore clear that the spin-label molecules do not adsorb on the surface of the Au nanoparticles in the fully stretched conformation. The length of the triphenylphosphine molecule adsorbed on Au is ca. 0.7 nm. Our data thus suggest that, for both spin-labeled particles **3a**,**b**, the nitroxide group is positioned immediately above the surface of the triphenylphosphine layer. To test the feasibility of such conformations, we performed simple molecular modeling. The molecule of disulfide **2b** was arbitrarily bent above the layer of triphenylphosphine on the Au surface, and the system was locally minimized. The resulting

TABLE 2: Calculated and Experimental d_1/d Parameters for Spin-Labeled Au Nanoparticles

spin labels per Au atom (N_r/N_{at})	average coverage $\bar{y}$	ligand **2a** exptl d_1/d	ligand **2a** calcd d_1/d	ligand **2a** length of spin label l, nm	ligand **2b** exptl d_1/d	ligand **2b** calcd d_1/d	ligand **2b** length of spin label l, nm
0.0012	0.11	0.54	0.52	0.80[a]	0.53	0.52	0.88[a]
0.0048	0.43	0.55	0.53		0.51	0.53	
0.0083	0.74	0.55	0.54		0.54	0.54	
0.012	1.06	0.59	0.56		0.56	0.55	
0.019	1.70	0.61	0.59		0.6	0.58	
0.024	2.13	0.63	0.61		0.61	0.60	
0.030	2.66	0.64	0.65		0.62	0.62	
0.036	3.19	0.66	0.68		0.64	0.65	
0.048	4.25	0.67	0.76	(1.02)[b]	0.64	0.72	(1.14)[b]
0.059	5.31	0.7	0.85	(1.12)[b]	0.64	0.80	(1.32)[b]

[a] Optimized length for all coverages except two bottom rows. [b] Optimized length for this coverage only.

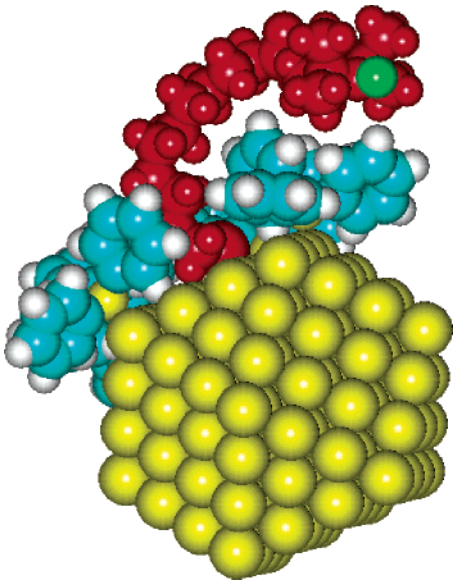

Figure 8. A possible conformation of ligand **2b** bending above the layer of triphenylphosphine. Ligand **2b** is shown in red, and the oxygen atom of the nitroxide functionality is colored green. The Au particle is a full-shell truncated octahedron and consists of 147 atoms. Four molecules of triphenylphosphine and 1 molecule of ligand **2b** were then placed on the particle terrace. The molecule of ligand **2** was arbitrarily bent above the layer of triphenylphosphine, and the structure was minimized locally.

structure (Figure 8) helps to visualize a possible conformation of the spin-labeled ligand.

The bent conformation of the spin labels is unexpected. Ligands are usually well-packed on the surface of Au nanoparticles, and they are commonly assumed to stretch away from the nanoparticle surface. In our case, however, the spin-labeled ligands are protruding above the layer of triphenylphosphine and hence have the freedom to bend. The conformation of such protruding ligands depends on the fine balance of the energy of solvation and the intermolecular interactions. The bent conformation could be stabilized by any unfavorable interactions between the solvent and the chain of the spin-labeled ligand or favorable interactions between the nitroxide group and the phenyl ring of the triphenylphosphine ligands. An additional driving force for bending the spin label could be the minimization of the particle size (e.g., to reduce the energy of tumbling in solution). One should note, however, that our data were obtained for frozen solutions. Although the samples were frozen quite rapidly, the rate of freezing was certainly slow on the conformation rearrangement time scale. It is therefore possible that, while the spin label exists in a bent conformation in a frozen sample, its solution conformation is different.

B. Model Validity. We made a number of assumptions in developing the analysis of d_1/d values, and it is instructive to test their validity and their effect on the results of our calculations. The most important assumptions were (a) the Au nanoparticles are spherical, (b) the distribution of particle sizes is Gaussian, (c) the ligands adsorb randomly on the surface, (d) the exchange interactions are negligible, and (e) the dipole−dipole interactions are dominated by the interactions between the nearest-neighboring spin labels.

The shape of Au nanoparticles has been a subject of much debate, involving both theoreticians and experimentalists. The particles are certainly not spherical; a number of possible shapes have been proposed for the magic-number Au particles (e.g., truncated octahedral, icosahedral, dodecahedral, etc.[22]). The relative contribution of non-magic-number particles and the number of defect sites on the particles cannot be quantified. The particles studied here are quite small and hence do not possess large terrace sites; we believe therefore that a spherical shape is a good approximation. To test if the width of the particle size distribution has a major impact on the results of our calculations, we simulated the d_1/d ratios for a series of Au nanoparticles possessing the same average radius as the ones used in this study, but a different width of size distribution. Interestingly, we found that our results are almost independent of the width of the size distribution up to the standard deviation of ca. 0.15 nm. This suggests that the d_1/d values do not show a strong dependence on the shape of the particle size distribution, and any errors caused by the deviation of the real distribution from the Gaussian should be small.

The assumption that the spin-labeled ligands adsorb randomly on the nanoparticle surface would be very interesting to test. The nonequivalence of binding sites on the Au surface would suggest that the distribution of spin-labeled ligands is not even, particularly at higher coverage. Unfortunately, our system does not allow us to determine the location of spin labels on the nanoparticle surface. We believe that even if the ligands do not adsorb randomly, the flexibility of the alkane chain in the molecules of **2a** and particularly **2b** will make the distribution of nitroxides fairly random. We can however deduce that the adsorption of the spin labels is not cooperative, and the spin-labeled ligands do not form homogeneous domains on the nanoparticle surface. Adsorption of pairs of spin labels would give strong coverage-independent dipole−dipole interactions, particularly at lower coverage. This is not observed. Cooperative adsorption of spin labels in domains should give very short average distances between nearest neighbors for particles with

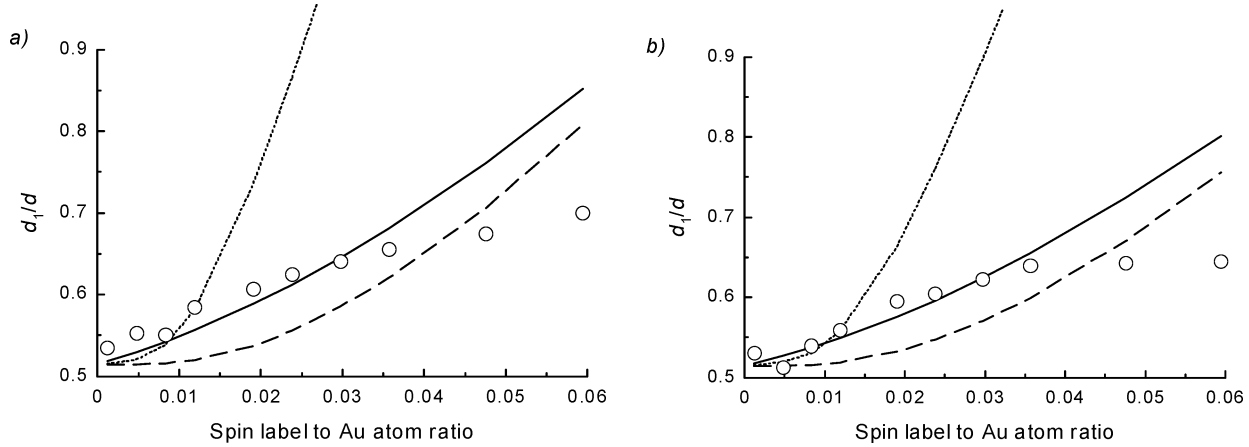

Figure 9. Experimental and simulated d_1/d values for spin-labeled nanoparticles **3a** (a) and **3b** (b). The solid line corresponds to the optimized simulation for all data points except the last two points. The dashed line assumes that particles of equal size have equal numbers of spin labels. The dotted line assumes that all particles are of the same size and have the same number of spin labels.

moderately average coverage (2−3 spin labels per particle). The data in Tables 1 and 2 clearly show that this does not happen.

To test if the shape of the spin-label distribution on the nanoparticle surface makes a strong impact on the results of our calculations, we simulated the d_1/d ratios with several simplifications to our model. The results are graphically shown in Figure 9a,b. The solid line shows the results of full simulation (the same data as in Table 2) optimized for all data points except the two highest coverages (vide infra). The dotted line was obtained for a system with no distribution of spin labels (e.g., all particles of equal size have an equal number of spin labels). The dashed line corresponds to an idealized system with all Au nanoparticles possessing the same size and the same number of spin labels. One can see that a nonsimplified simulation gives a much better fit. This supports the validity of our assumptions.

The question of exchange interactions between nearest neighbors is also very interesting. Exchange interaction can only be ignored for distances larger than ca. 1 nm.[8] The average distance between spin labels for the higher-coverage particles (last two−three entries in Table 1) is ca. 1.5 nm. It is likely that in these particles a substantial number of spin labels will be closer than 1 nm to each other, and hence, the exchange interaction between them can no longer be ignored. The data in Figure 9 and Table 2 show that the simulated d_1/d's for the two highest coverages substantially deviate from the experimental data. We believe exchange interaction in these nanoparticles is at least partially responsible for this deviation.

Our assumption that only the nearest-neighboring spin labels contribute to the dipole−dipole interaction could also explain exaggerated values of the calculated d_1/d parameters at high coverage. While this is probably a very good approximation for low coverage, the interactions at high coverage are likely to involve whole domains of adjacent spin labels rather than pairs of nearest neighbors. We would expect, however, the effect of next (and further) nearest neighbors to be rather small. The problem of dipole−dipole interactions in domains of spin labels is also present in our model calibration system (bulk TEMPO solutions); one could therefore expect the contributions of next-nearest neighbors to the model system and to Au nanoparticles to be similar, and hence, the errors caused by ignoring these interactions will be reduced.

Alternatively, the poor fit of calculated d_1/d values at high coverage could be explained by the steric interactions between spin labels. This effect should be particularly important for disulfide **3b**. At high coverage, there will be a number of spin labels adsorbed on the same particle. There will simply not be enough space on the nanoparticle surface to allow all these ligands to bend. Some ligands will therefore have to change their conformations to more extended ones. The calculated d_1/d parameters match experimental values for the penultimate and highest-coverage data points for spin label **2a** if the length of the molecule is 1.02 and 1.12 nm, respectively. This length is quite reasonable; it is greater than that of the "bent" molecule, yet shorter than the fully extended one. Similarly, the length of spin label **2b** is 1.14 and 1.32 nm for the penultimate and highest-coverage data points, respectively. One can see that these numbers are again within the reasonable range; the deviation from the "bent" conformation is substantially greater for spin label **2b** than for spin label **2a**.

IV. Conclusions

We have developed a method to analyze dipole−dipole interactions in EPR spectra of frozen solutions of spin-labeled nanoparticles. Our method relies on the empirical d_1/d parameter to characterize the dipolar line broadening and takes into account the interactions between nearest-neighboring spin labels which are adsorbed randomly on the surface of spherical Au nanoparticles. The model further assumes a Gaussian distribution of nanoparticle size.

Application of this analysis to two types of spin-labeled nanoparticles showed that, for nanoparticles protected by a mixture of two ligands with different chain length, the longer ligand is not extended fully into solution but instead wraps around the nanoparticle to minimize its size. This is an interesting observation which contrasts with a commonly accepted view that the alkane chains are fully extended in monolayers. Mixed layers of short- and long-chain ligands (similar to the ones studied in this work) are often used to anchor bulky molecules to the surface; it is usually assumed that the long ligands protrude high above the monolayer surface. Our observations suggest that this is not always the case. It would be important to see if these findings are also applicable to the monolayers on planar surfaces and other supramolecular/nanoscale assemblies.

We have also shown that the spin-labeled ligands do not adsorb cooperatively on the surface of Au nanoparticles and there is no phase separation of the ligands on the surface; our system, however, could not probe whether the spin labels are adsorbed randomly on the nanoparticles.

It is important to mention that the organization of organic ligands on the Au nanoparticle surface is very difficult to probe

using other methods, and such studies are hence very rare. While a number of techniques have been successfully used to measure the particle size and the composition of the organic shell, the information about the distribution of ligands on the nanoparticle surface and the conformation and the dynamics of the organic layer remains elusive. We are confident that the spin-labeling methods will contribute substantially to our understanding of organization of molecules on the Au nanoparticle surface and other interfaces.

V. Experimental Section

Triphenylphosphine-protected Au nanoparticles **1** were prepared by a modified procedure of Hutchinson et al.[23] The nanoparticles were kept as crude reaction mixtures which were purified by GPC immediately before use. Spin labels **2a**,**b** were prepared as described elsewhere.[9] Spin-labeled nanoparticles **3a**,**b** were prepared by mixing the solutions (4/1 toluene/DCM) of the spin labels **2a**,**b** ($10^{-3}-10^{-4}$ M) and Au nanoparticles **1** ($5\cdot10^{-4}$ M) in the desired proportion. The reaction mixtures were left overnight at room temperature. For lower coverage nanoparticles (up to 5 spin labels per particle), the crude reaction mixtures were used without purification. For higher coverage, the reaction mixtures were separated by preparative GPC using a short (30-cm) column packed with BioBeads SX-1 gel. The samples for ICP−OES analysis were digested in aqua regia. TEM images were recorded on a JEOL 1200 EX instrument. Particle size and size distribution were determined by measuring the radii of 250−300 randomly chosen particles using *ImageJ* software.[24] EPR spectra were recorded on a JEOL JES-RE1X instrument at the X-band using a 100-kHz modulation frequency.

Acknowledgment. The authors acknowledge EPSRC (GR/S45300/01) and NATO (PST.EV.980030) for funding. We thank Dr A. C. Whitwood for help with instrumentation and discussions.

Supporting Information Available: Full details of mathematical analysis of average distance between nearest neighbors on a sphere; average nanoparticle coverage as a function of particle size; number of Au atoms at the nanoparticle surface; and EPR spectral simulations for spin-labeled nanoparticles. This material is available free of charge via the Internet at http://pubs.acs.org.

References and Notes

(1) For recent reviews, see: Templeton, A. C.; Wuelfing, W. P.; Murray, R. W. *Acc. Chem. Res.* **2000**, *33*, 27. Bönnemann, H.; Richards, R. M. *Eur. J. Inorg. Chem.* **2001**, 2455. Schmid, G.; Corain, B. *Eur. J. Inorg. Chem.* **2003**, 3081. Daniel, M.-C.; Astruc, D. *Chem. Rev.* **2004**, *104*, 293.

(2) Brust, M.; Walker, M.; Bethell, D.; Schiffrin, D. J.; Whyman, R. *J. Chem. Soc., Chem. Commun.* **1994**, 801.

(3) Badia, A.; Gao, W.; Singh, S.; Demers, L.; Cuccia, L.; Reven, L. *Langmuir* **1996**, *12*, 1262.

(4) Badia, A.; Cuccia, L.; Demers, L.; Morin, F.; Lennox, R. B. *J. Am. Chem. Soc.* **1997**, *119*, 2682.

(5) Song, Y.; Murray, R. W. *J. Am. Chem. Soc.* **2002**, *124*, 7096.

(6) Ionita, P.; Caragheorgheopol, A.; Gilbert, B. C.; Chechik, V. *Langmuir* **2004**, *20*, 11536.

(7) Hostetler, M. J.; Templeton, A. C.; Murray, R. W. *Langmuir* **1999**, *15*, 3782.

(8) Easton, S. S.; Eaton, G. R. *Distance Measurements in Biological Systems by EPR*; Berliner, L. J., Reuben, J., Eds; Biological Magnetic Resonance Series Vol. 19; Kluwer Academic/Plenum Publishers: New York, 2000.

(9) Chechik, V.; Wellsted, H. J.; Korte, A.; Gilbert, B. C.; Caldararu, H.; Ionita, P.; Caragheorgheopol, A. *Faraday Discuss.* **2004**, *125*, 279.

(10) Ionita, P.; Caragheorgheopol, A.; Gilbert, B. C.; Chechik, V. *J. Am. Chem. Soc.* **2002**, *124*, 9048.

(11) Chechik, V. *J. Am. Chem. Soc.* **2004**, *126*, 7780.

(12) Warner, M. G.; Reed, S. M.; Hutchison, J. E. *Chem. Mater.* **2000**, *12*, 3316.

(13) Risse, T.; Hill, T.; Schmidt, J.; Abend, G.; Hamann, H.; Freund, H.-J. *J. Phys. Chem. B* **1998**, *102*, 2668.

(14) Steinhoff, H. J.; Radzwill, N.; Thevis, W.; Lenz, V.; Brandenburg, D.; Antson, A.; Dodson, G.; Wollmer, A. *Biophys J.* **1997**, *73*, 3287.

(15) Rabenstein, M. D.; Shin, Y.-K. *Proc. Natl. Acad. Sci. U.S.A.* **1995**, *92*, 8239. Steinhoff, H.-J. *Front. Biosci.* **2002**, *7*, c97, 43. Steinhoff, H.-J.; Dombrowsky, O.; Karim, C.; Schneiderhahn, C. *Eur. Biophys. J.* **1991**, *20*, 293. Hustedt, E. J.; Beth, A. H. *Annu. Rev. Biophys. Biomol. Struct.* **1999**, *28*, 129.

(16) Kokorin, A. I.; Zamaraev, K. I.; Grigoryan, G. L.; Ivanov, V. P.; Rozantsev, E. G. *Biofizika* **1972**, *17*, 34 (in Russian). Likhtenshtein, G. I. *Spin Labeling Methods in Molecular Biology*; Wiley & Sons: New York, 1976. Likhtenshtein, G. I. *Biophysical Labeling Methods in Molecular Biology*; Cambridge University Press: New York, 1993. Kulikov, A. V.; Likhtenstein, G. I. *Adv. Mol. Relax. Interact. Processes* **1997**, *10*, 47. Kokorin, A. I. Dr. Thesis. N. N. Semenov Institute of Chemical Physics, Moscow, 1973 (in Russian).

(17) Chandrasekhar, S. *Rev. Mod. Phys.* **1943**, *15*, 1.

(18) We estimate the error of experimental d_1/d values to be approximately 0.01.

(19) Scott, D.; Tout, C. A. *Mon. Not. R. Astron. Soc.* **1989**, *241*, 109.

(20) Schaaff, T. G.; Shafigullin, M. N.; Khoury, J. T.; Vezmar, I.; Whetten, R. L.; Cullen, W. G.; First, P. N.; Gutíerrez-Wing, C.; Ascencio, J. A.; José-Yacamán, M. *J. Phys. Chem. B* **1997**, *101*, 7885.

(21) Strictly speaking, the integration interval should be from 0 to $+\infty$, as the particle radius cannot be negative. However, as the particles have relatively low polydispersity, the probability of finding particles with $R \approx 0$ is very small. Hence, integration from $-\infty$ to $+\infty$ will not introduce a large error.

(22) Cleveland, C. L.; Landman, U.; Schaaff, T. G.; Shafigullin, M. N.; Stephens, P. W.; Whetten, R. L. *Phys. Rev. Lett.* **1997**, *79*, 1873. Doye, J. P. K.; Wales, D. J. *J. Chem. Soc., Faraday Trans.* **1997**, *93*, 4233. Rapoport, D. H.; Vogel, W.; Cölfen, H.; Schlögl, R. *J. Phys. Chem. B* **1997**, *101*, 4175. Alvarez, M. M.; Khoury, J. T.; Schaaff, T. G.; Shafigullin, M. N.; Vezmar, I.; Whetten, R. L. *Chem. Phys. Lett.* **1997**, *266*, 91. Whetten, R. L.; Khoury, J. T.; Alvarez, M. M.; Murthy, S.; Vezmar, I.; Wang, Z. L.; Stephens, P. W.; Cleveland, C. L.; Luedtke, W. D.; Landman, U. *Adv. Mater.* **1996**, *8*, 428.

(23) Weare, W. W.; Reed, S. M.; Warner, M. G.; Hutchinson, J. E. *J. Am. Chem. Soc.* **2000**, *122*, 12890−12891.

(24) Kuzmic, P. *Anal. Biochem.* **1996**, *237*, 260. The free software can be downloaded from http://www.biokin.com/dynafit.